Atmos. Chem. Phys., 10, 5707–5718, 2010
www.atmos-chem-phys.net/10/5707/2010/
doi:10.5194/acp-10-5707-2010

Atmospheric Chemistry and Physics

Molecular hydrogen (H_2) emissions and their isotopic signatures (H/D) from a motor vehicle: implications on atmospheric H_2

M. K. Vollmer[1], **S. Walter**[2], **S. W. Bond**[1], **P. Soltic**[3], **and T. Röckmann**[2]

[1]Empa, Swiss Federal Laboratories for Materials Science and Research, Laboratory for Air Pollution and Environmental Technology, Überlandstrasse 129, 8600 Dübendorf, Switzerland
[2]Institute for Marine and Atmospheric research Utrecht, Utrecht University, Princetonplein 5, 3508TA Utrecht, The Netherlands
[3]Empa, Swiss Federal Laboratories for Materials Science and Research, Laboratory of I. C. Engines, Überlandstrasse 129, 8600 Dübendorf, Switzerland

Received: 24 November 2009 – Published in Atmos. Chem. Phys. Discuss.: 5 February 2010
Revised: 26 May 2010 – Accepted: 10 June 2010 – Published: 29 June 2010

Abstract. Molecular hydrogen (H_2), its isotopic signature (deuterium/hydrogen, δD), carbon monoxide (CO), and other compounds were studied in the exhaust of a passenger car engine fuelled with gasoline or methane and run under variable air-fuel ratios and operating modes. H_2 and CO concentrations were largely reduced downstream of the three-way catalytic converter (TWC) compared to levels upstream, and showed a strong dependence on the air-fuel ratio (expressed as lambda, λ). The isotopic composition of H_2 ranged from δD=−140‰ to δD = −195‰ upstream of the TWC but these values decreased to −270‰ to −370‰ after passing through the TWC. Post-TWC δD values for the fuel-rich range showed a strong dependence on TWC temperature with more negative δD for lower temperatures. These effects are attributed to a rapid temperature-dependent H-D isotope equilibration between H_2 and water (H_2O). In addition, post TWC δD in H_2 showed a strong dependence on the fraction of removed H_2, suggesting isotopic enrichment during catalytic removal of H_2 with enrichment factors (ε) ranging from −39.8‰ to −15.5‰ depending on the operating mode. Our results imply that there may be considerable variability in real-world δD emissions from vehicle exhaust, which may mainly depend on TWC technology and exhaust temperature regime. This variability is suggestive of a δD from traffic that varies over time, by season, and by geographical location. An earlier-derived integrated pure (end-member) δD from anthropogenic activities of −270‰ (Rahn et al., 2002) can be explained as a mixture of mainly vehicle emissions from cold starts and fully functional TWCs, but enhanced δD values by >50‰ are likely for regions where TWC technology is not fully implemented. Our results also suggest that a full hydrogen isotope analysis on fuel and exhaust gas may greatly aid at understanding process-level reactions in the exhaust gas, in particular in the TWC.

Correspondence to: M. K. Vollmer
(martin.vollmer@empa.ch)

1 Introduction

The poorly understood budget of atmospheric molecular hydrogen (H_2) has received increased attention over the past years because of a potentially massive disturbance in the near future due to a potential shift towards a hydrogen energy economy. Recent studies have revealed potential negative impacts on stratospheric ozone and on earth's climate systems via the role of H_2 in atmospheric chemistry; however, quantitative estimates are highly uncertain, largely due to unknown leakage rates of H_2 to the atmosphere from future H_2 energy systems. In the traffic sector, current H_2 emissions from conventional combustion engine systems would disappear, but could be replaced by leakage and purged losses from H_2-powered vehicles.

H_2 is abundant in the atmosphere at relatively high concentrations (hereafter expressed as dry air mole fraction) of 450 ppb – 550 ppb (parts-per-billion, 10^{-9}, molar). Its source and sink strengths are given here as ranges found in the literature (Novelli et al., 1999; Hauglustaine and Ehhalt, 2002; Sanderson et al., 2003; Rhee et al., 2006; Price et al., 2007; Xiao et al., 2007; Ehhalt and Rohrer, 2009): The major

sources are in-situ photochemical production from methane (CH_4) and other hydrocarbons (30–77 Tg a^{-1}), fossil fuel emissions (11–20 Tg a^{-1}), biomass burning (10 – 20 Tg a^{-1}), and minor emissions from microbial nitrogen (N_2) fixation on land and in the oceans (6–10 Tg a^{-1}). The dominant sink of H_2 is enzymatic destruction in soil (55–88 Tg a^{-1}), but there is also considerable removal through oxidation by the hydroxyl radical in the atmosphere (15–19 Tg a^{-1}). These fluxes result in a tropospheric lifetime of H_2 of 1.4–2.2 a. Due to the dominant soil sink and the larger land coverage in the Northern Hemisphere, this hemisphere exhibits smaller tropospheric concentrations compared to the Southern Hemisphere, which is an unusual distribution for atmospheric trace gases.

Stable isotope measurements of H_2 using the hydrogen/deuterium (H/D) ratio have greatly added to differentiating various sources and sinks (Brenninkmeijer et al., 2003; Ehhalt and Rohrer, 2009). This is particularly true because of largely differing isotopic signatures of the sources. For example, H_2 from CH_4 oxidation is particularly enriched in deuterium with δD values ∼130‰ to 180‰ (Rahn et al., 2003; Rhee et al., 2006; Feilberg et al., 2007; Röckmann et al., 2003; Pieterse et al., 2009), biogenic H_2 is extraordinarily depleted ($\delta D \sim -700$‰, e.g. Rahn et al. (2002); Walter and et al. (2010)), and combustion-derived H_2 has δD values of approximately −170‰ to −270‰ (Gerst and Quay, 2001; Rahn et al., 2002).

Automobile exhaust is believed to dominate anthropogenic H_2 emissions, and has recently been estimated globally at 4.2–5.4 Tg a^{-1} with a decreasing trend, based on a fleet-integrated tunnel emission study (Vollmer et al., 2007). The single available isotope study of regional traffic emissions using polluted air samples from the Los Angeles basin by Rahn et al. (2002) suggests an urban pollution isotopic signature of −270‰ for this region. Samples taken near the exhaust of individual vehicles in their study showed considerable variability in the isotopic signature, as did a few samples collected in a parking garage by Gerst and Quay (2001), which showed less depleted δD.

Engine and catalytic converter technology is evolving rapidly, and along with the increasing diversity of fuel types, presents a challenge for vehicle emissions characterization. Such studies can be conducted on various levels of detail, and range from regional scale atmospheric observations of polluted air masses to single unit process studies. Isotope investigations can greatly improve the distinction from other sources and sinks of pollutants. For vehicle exhaust, progress has recently been achieved through isotopic studies of e.g. carbon monoxide, CO (Tsunogai et al., 2003), methane, CH_4 (Chanton et al., 2000; Nakagawa et al., 2005), and nitrous oxide, N_2O (Toyoda et al., 2008). Here we present results from a study on a passenger car engine for which we have measured pre- and post-catalytic H_2 concentrations and – to our knowledge for the first time – H/D signatures under variable engine and fuel settings.

2 Materials and methods

2.1 Experimental setup

The engine experiment was conducted in 2008 on an engine test bench at the Empa Internal Combustion Engines Laboratory using a naturally-aspirated passenger car engine with four cylinders, 2-L displacement, and the capability to combust either gasoline or natural gas. The engine was equipped with a state-of-the art engine control unit, which was originally calibrated to achieve Euro-4 emission limits for a mid-size passenger car. On the test bench, the control parameters could be modified to study e.g. the influence of the air-to-fuel ratio on combustion and emissions. The combustion air fed to the engine was conditioned to a temperature of 295 K and a relative humidity of 50%. The exhaust system was equipped with a single three-way ceramic substrate catalytic converter (TWC) with a cell density of 600 cells per square inch (cpsi) and coated with palladium and rhodium as the catalytically active materials. Ceria, an oxide of the element cerium, was used in the TWC's wash-coat to achieve the desired oxygen storage capacity. For the sake of the later temperature discussion, it is worthy to mention that a TWC is not actively heated but that it is initially cold (termed "cold start" in traffic studies) after engine start-up until sufficient hot exhaust gas passes through it to make it fully functional (light-off temperature). For air-to-fuel ratio feedback control, the engine was equipped with a linear lambda (λ) sensor upstream of the catalyst and a switching-type λ sensor downstream of the TWC for bias control. Linear λ sensors are able to measure deviations of λ very precisely but they unfortunately show a relatively slow signal drift, which depends on many factors. To compensate for this drift, the bias of the linear λ sensor is corrected occasionally using the signal of a much simpler switching-type λ sensor mounted downstream of the TWC. Such switching-type sensors show a very stable and steep signal change at λ=1 but no useful information of the actual λ value in fuel-rich or fuel-lean operating conditions. The engine control used a square signal "λ-wobbling" function with an amplitude of 0.02 to the nominal λ setting. These rich-lean excursions are very often used in modern engine controls to enhance the TWC's efficiency, and to perform diagnosis of the TWC during engine operation using the TWC's dynamic response to this wobbling.

The experiment was conducted for 4 different operating modes (OMs) as is shown in Table 1, where OM-1 used the same engine settings as OM-2, but in the first case the TWC was cooled by active air ventilation of the exhaust manifold and the piping upstream of the TWC. All OMs reflect relatively low engine power, which are frequently used in normal operations of passenger cars. OM-2 is a standard setting, which is widely used in engine research for comparative purposes. OM-3 and OM-4 differ from OM-2 in torque and crankshaft speed and represent low revolution per minute (rpm) and high-rpm driving, both at double the engine power

Table 1. Operating modes (OM) for the experiments conducted on a passenger car engine. The three-way catalytic converter (TWC) was actively cooled in operating mode 1. OM-1 through OM-4 are gasoline-fuelled, OM-3-CH4 is methane-fuelled. Upstream and downstream TWC temperatures are lambda-dependent (low temperatures for low lambda). Although the TWC is not actively heated, some downstream temperatures are higher due to exothermic reactions occurring within the TWC.

Operating Mode (OM)	Crankshaft speed [r.p.m]	Torque [N m]	Power [kW]	Downstream TWC cooling	Upstream TWC temperature range [°C]	Downstream TWC temperature range [°C]
OM-1	2000	31.6	6.6	yes	460–490	456–534
OM-2	2000	31.6	6.6	no	530–556	512–586
OM-3	2000	63.2	13.2	no	598–629	566–642
OM-4	4000	31.6	13.2	no	690–721	665–753
OM-3-CH_4	2000	63.2	13.2	no	566–590	558–620

of OM-1 and OM-2. In order to study the air-to-fuel settings on the pollutant emissions before and after TWC, the λ for each OM was varied around $\lambda = 1.0$. To prevent undesired fuelling changes caused by a λ bias control, bias control was turned off. The gasoline used for these experiments was market fuel with research octane number 95.5, a density of 736 kg m^{-3}, a sulphur content of 22.6 mg kg^{-1}, and an H/C ratio of 1.97. One of the purposes of this experiment was to study the interference of H_2 in the exhaust on the lambda probe. For this reason all operating modes were repeated using CH_4 as the engine fuel (commercial bottled CH_4 based on fossil-fuel natural gas). However, the focus of the H_2 stable isotope study was on the exhaust of the gasoline-powered engine, and we therefore discuss the CH_4 results only briefly in the context of the H_2 isotopes. In addition to the chemical species discussed here, measurements in the exhaust were made of O_2, nitrogen oxides (NO_x, NO, NO_2), CH_4, short-chained hydrocarbons (C_2–C_4), some aromatics, total hydrocarbons (HC), water (H_2O), N_2O, and sulphur dioxide (SO_2).

Samples for D/H isotope analysis were collected at ∼2 bar in 1-L glass flasks fitted with 2 stopcocks (NORMAG, Illmenau, Germany), and others at ∼3 bar in ∼2-L internally electro-polished stainless steel (ss) canisters using a small membrane pump (KNF model N86-KTE). The sampling stream was cooled in an ice bath before entering the pump and the condensed water was periodically removed. The samples were further dried using magnesium perchlorate ($Mg(ClO_4)_2$) before collection in the flasks. Analysis of the samples was performed within 3 months after their collection.

2.2 Instrumentation

H_2 concentrations were measured on-line using a commercially available electron impact ionization mass spectrometer (EIMS, H-Sense, V&F Analyse und Messtechnik, Absam, Austria). The instrument precision is ∼1% (1σ of 1-min mean). However the measurements were affected by a blank of ∼8 ppm (parts-per-million, 10^{-6}, molar), likely caused by some H_2O interference in the system. This blank was determined and corrected for by comparing the EIMS results with the concentration results from the flask samples, which were available for the low-concentration range ($\lambda > 1$). While this blank correction is of little relevance for the high-concentration samples, it resulted in considerable uncertainties of up to 50% for some of the low-concentration samples. Calibration of the instrument was achieved using commercial standards (30 ppm and 1000 ppm, Messer Schweiz, accuracies 0.5%) and during an independent validation study, the instrument was found to exhibit linear response within the range of our measured concentrations (Brühlmann, 2004). Overall accuracies of the H_2 concentrations are estimated at 5 ppm or 3%, whichever is greater.

CO, CO_2, and H_2O were measured on-line using an automotive Fourier Transformation Infra-red (FTIR) instrument (AVL SESAM). This instrument was calibrated during commissioning using high-precision gases and did not need recalibration during the experiment. Estimated uncertainties are 0.14% for H_2O, 0.12% for CO and 0.33% for CO_2. The CO and CO_2 concentrations were converted to dry air mole fractions using this instrument's H_2O results. Earlier-mentioned compounds, which are not discussed here, were also measured on this FTIR and on a standard engine emission bench instrument (Horiba Mexa 9200).

Isotopic measurements of H_2 from the flask samples were conducted in the isotope laboratory of the Institute for Marine and Atmospheric research Utrecht (IMAU), Utrecht University using isotope ratio mass spectrometry (Rhee et al., 2004). Isotope results are reported using the "delta" notation, $\delta D = [(D/H)_s/(D/H)_{VSMOW} - 1] \times 1000‰$, where s is the H_2 of the sample and VSMOW is Vienna standard mean ocean water used as reference (Craig, 1961; Gonfiantini, 1978). The mean of the 1-σ precisions from repeated analysis and duplicate samples is 11‰, which is poorer than for ambient air measurements and caused by the high concentrations employed in this study.

2.3 Results and discussion

The results for our compounds of interest are listed in Table 2 and shown in Fig. 1 as a function of the air-fuel ratio. The air-fuel ratio is expressed here as a lambda (λ) value, whereby $\lambda < 1$ is the range of fuel-rich combustion (typically during vehicle accelerations) and $\lambda > 1$ corresponds to fuel-lean combustion (excess oxygen present). H_2 and CO are produced during incomplete combustion, and their abundance is related, amongst other chemical reactions, through the water-gas shift reaction $H_2 + CO_2 \leftrightarrow H_2O + CO$. Pre-TWC results showed largest emissions under fuel-rich conditions, with concentrations up to ∼14 000 ppm for H_2 and ∼41 000 ppm for CO. These concentrations decreased with increasing λ to about 1000–1500 ppm for H_2 and 4000–7000 ppm for CO for the leanest samples. From the presence of large H_2 concentrations in all pre-TWC samples, we conclude that the H_2 concentration and isotope ratio in the intake air (which we measured in a nearby ambient sample with a concentration of 573 ppb and a δD of 83.3‰) is not relevant in the following discussion.

Post-TWC emissions of H_2 and CO were lower compared to the pre-TWC emissions. Here the emissions were also larger in the fuel rich range, but nearly disappeared in the fuel-lean range. For H_2, most concentrations of the fuel-lean experiments were below typical ambient atmospheric values of ∼0.5 ppm, implying that under these conditions, H_2 is destroyed on the TWC. The post-TWC H_2 concentrations in the fuel-rich range were highly dependent on the operating mode, with highest emissions for OM-4. In contrast, the post-TWC concentrations for CO showed remarkably similar λ dependence for all 4 operating modes.

The cooling of the TWC also had significant effects on post-TWC H_2 emissions. The reduction of the TWC temperatures in OM-1 by ∼ 50°C compared to OM-2 (Table 1) resulted in a reduction of H_2 emissions to less than half of those in the fuel-rich range, but had no effect on the CO emissions. These observations demonstrate that reactions other than the water-gas-shift play a role, because the latter alone would be driving the equilibrium to higher H_2 yield at reduced temperatures (Haryanto et al., 2009), and not the opposite we've observed. One possible explanation for these observations is that the TWC's active sites are occupied by hydrocarbons thereby preventing adsorption of H_2O required for the water-gas-shift reaction (e.g. Auckenthaler, 2005).

Our D/H isotope analysis shows largely differing isotope ratios between the individual settings, with the following three major observations. Firstly, for a given air-fuel ratio, the H_2 in the post-TWC exhaust was more depleted in deuterium compared to the pre-TWC exhaust. For the range where pre- and post-TWC samples were available, the pre-TWC δD values ranged from −140‰ to −195‰ but these values decreased to between −270‰ and −370‰ after passing through the TWC. Secondly, the post-TWC D/H ratios showed a strong dependence on λ with lower δD in the fuel-

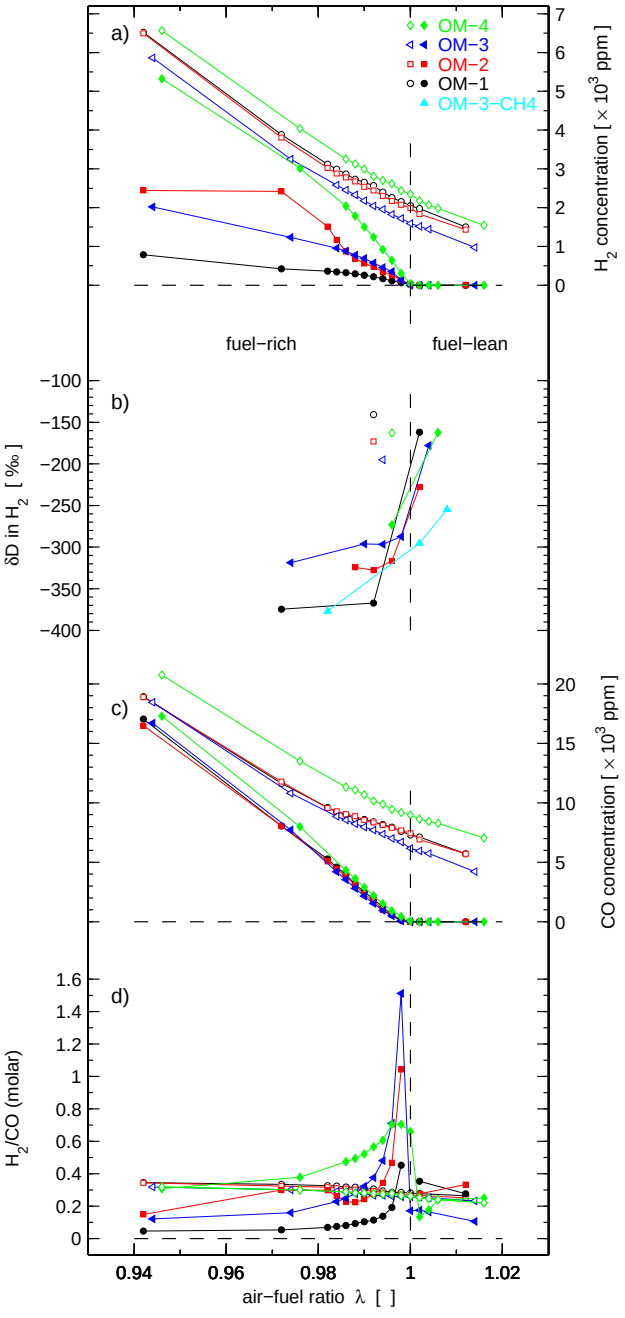

Fig. 1. Engine exhaust concentrations for H_2 **(a)** and its isotope ratio δD **(b)**, CO **(c)**, and the ratio H_2/CO **(d)** vs. the air-fuel ratio (λ) upstream (open symbols) and downstream (filled symbols) of the three-way catalytic (TWC) converter. The colors differentiate the four main operating modes of the gasoline-fuelled engine and the isotope results for one methane-fuelled operating mode in (b). The data for the lowest λ are omitted to show the remaining results in closer detail. Vertical and horizontal dashed lines are visual aids at λ=1 and zero y-values, respectively.

Table 2. Temperatures, trace gas concentrations, and H_2 isotope ratio for pre-TWC (three-way catalytic converter) and post-TWC exhaust gasoline and from a methane-fuelled engine. The operating modes (OM) OM 1–4 are gasoline fuelled and OM 3-CH4 is methane fuelled. These OM are further specified in Table 1.

		Pre-TWC					Post-TWC				
Operating Mode	Lambda [ ]	Temp. [°C]	H_2 conc. [10^3 ppm]	δD-H_2 [‰]	CO conc. [10^3 ppm]	CO_2 conc. [10^3 ppm]	Temp. [°C]	H_2 conc [10^3 ppm]	δD-H_2 [‰]	CO conc. [10^3 ppm]	CO_2 conc [10^3 ppm]
1	0.892	466	13.91	–	38.86	122	456	9.37	–	37.93	124
1	0.942	481	6.52	–	18.93	139	483	0.79	–	17.03	143
1	0.972	485	3.88	–	11.63	145	504	0.42	–375	8.05	152
1	0.982	487	3.12	–	9.60	146	513	0.36	–	5.27	154
1	0.984	487	2.99	–	9.26	146	515	0.34	–	4.59	155
1	0.986	488	2.87	–	9.01	146	517	0.32	–	3.97	156
1	0.988	488	2.73	–	8.64	147	520	0.29	–	3.17	156
1	0.990	488	2.65	–	8.61	147	523	0.26	–	2.51	156
1	0.992	490	2.57	–141	8.41	147	525	0.22	–367	1.92	157
1	0.994	489	2.40	–	8.17	147	528	0.17	–	1.23	157
1	0.996	490	2.26	–	7.94	147	530	0.11	–	0.60	158
1	0.998	490	2.15	–	7.59	147	532	0.06	–	0.14	157
1	1.000	490	2.05	–	7.30	147	534	0.02	–	0.00	157
1	1.002	490	1.98	–	7.13	147	531	0.00	–162	0.00	157
1	1.012	491	1.50	–	5.71	148	521	0.00	–	0.00	155
2	0.892	530	13.92	–	39.18	122	512	9.58	–	37.80	123
2	0.942	545	6.50	–	18.89	139	537	2.44	–	16.48	143
2	0.972	551	3.81	–	11.78	145	556	2.42	–	8.06	152
2	0.982	553	3.03	–	9.56	146	563	1.51	–	5.08	155
2	0.984	554	2.88	–	9.28	146	566	1.17	–	4.45	155
2	0.986	553	2.78	–	9.04	146	567	0.87	–	3.82	156
2	0.988	555	2.68	–	8.87	147	569	0.69	–324	3.08	156
2	0.990	553	2.54	–	8.55	147	571	0.56	–	2.32	156
2	0.992	555	2.44	–173	8.35	147	576	0.48	–328	1.73	157
2	0.994	553	2.31	–	8.14	147	576	0.35	–	1.02	157
2	0.996	555	2.17	–	7.89	147	581	0.26	–317	0.56	157
2	0.998	555	2.08	–	7.67	147	580	0.14	–	0.13	157
2	1.000	556	1.99	–	7.45	147	586	0.02	–	0.00	157
2	1.002	555	1.83	–	6.90	147	580	0.00	–228	0.00	156
2	1.012	555	1.43	–	5.71	147	570	0.00	–	0.00	156
3	0.894	598	13.25	–	38.96	123	568	9.89	–	37.49	124
3	0.944	616	5.86	–	18.45	140	596	2.02	–	16.69	143
3	0.974	620	3.25	–	10.80	146	616	1.23	–319	7.73	153
3	0.984	624	2.58	–	8.85	148	627	0.96	–	4.20	156
3	0.986	623	2.45	–	8.55	148	627	0.88	–	3.53	156
3	0.988	623	2.33	–	8.24	148	629	0.78	–	2.81	156
3	0.990	625	2.18	–	7.96	148	632	0.69	–296	2.15	157
3	0.992	625	2.05	–	7.71	148	633	0.57	–	1.53	157
3	0.994	625	1.96	–195	7.36	149	634	0.46	–297	0.95	157
3	0.996	625	1.83	–	7.02	149	638	0.35	–	0.50	158
3	0.998	627	1.72	–	6.70	149	640	0.13	–287	0.08	157
3	1.000	625	1.59	–	6.16	149	638	0.00	–	0.00	157
3	1.002	626	1.52	–	5.95	149	638	0.00	–	0.00	157
3	1.004	626	1.44	–	5.74	150	635	0.00	–178	0.00	157
3	1.014	629	0.98	–	4.22	149	626	0.00	–	0.00	155
4	0.896	690	13.93	–	41.39	120	668	14.00	–	38.46	123
4	0.946	710	6.57	–	20.73	139	701	5.32	–	17.29	143
4	0.976	715	4.04	–	13.50	143	725	3.02	–	7.98	152
4	0.986	717	3.25	–	11.32	145	737	2.04	–	4.31	155
4	0.988	719	3.13	–	11.08	145	739	1.78	–	3.61	156
4	0.990	717	2.99	–	10.67	145	741	1.50	–	2.88	156
4	0.992	718	2.81	–	10.15	145	743	1.24	–	2.19	157
4	0.994	719	2.70	–	9.89	146	745	0.92	–	1.52	157
4	0.996	719	2.62	–163	9.44	146	749	0.64	–273	0.91	157
4	0.998	720	2.44	–	9.18	146	750	0.30	–	0.43	157
4	1.000	719	2.35	–	8.97	146	753	0.04	–	0.06	157
4	1.002	720	2.18	–	8.63	146	751	0.00	–	0.00	156
4	1.004	721	2.07	–	8.43	146	748	0.00	–	0.00	156
4	1.006	720	1.98	–	8.28	147	745	0.00	–162	0.00	156
4	1.016	720	1.54	–	7.04	147	735	0.00	–	0.00	155
3-CH4	0.902	566	24.35	–	35.52	88	567	19.32	–	34.14	92
3-CH4	0.952	583	12.33	–	19.46	102	586	3.74	–	15.62	107
3-CH4	0.982	588	6.33	–	10.99	108	608	0.76	–377	4.11	117
3-CH4	0.992	589	4.92	–	9.20	110	618	0.21	–	0.24	119
3-CH4	0.994	590	4.64	–	8.97	111	617	0.13	–	0.06	119
3-CH4	0.996	588	4.41	–	8.62	110	620	0.09	–	0.02	119
3-CH4	0.998	589	3.96	–	8.25	111	620	0.15	–	0.06	119
3-CH4	1.000	588	3.70	–	7.79	110	615	0.00	–	0.00	118
3-CH4	1.002	588	3.50	–	7.39	110	609	0.00	–295	0.00	118
3-CH4	1.004	590	3.34	–	7.19	111	603	0.00	–	0.00	117
3-CH4	1.006	588	3.08	–	6.69	111	596	0.00	–	0.00	117
3-CH4	1.008	589	3.05	–	6.75	111	589	0.00	–255	0.00	116
3-CH4	1.010	586	2.80	–	6.20	110	590	0.00	–	0.00	116
3-CH4	1.012	586	2.69	–	5.97	110	581	0.00	–	0.00	115
3-CH4	1.022	587	1.93	–	4.53	110	571	0.00	–	0.00	114

rich range (lowest δD values are −370‰) and higher δD in the fuel-lean range (up to $\delta D = -160$‰). Thirdly, we observed systematic differences between the operating modes, with OM-1 showing the lowest δD values and OM-4 exhibiting the highest δD values.

2.4 H_2 isotope equilibration with H_2O

The finding of lower isotope δD values after vs. before the TWC is opposite to what would be expected if H_2 was removed through a normal chemical (oxidation) process where the light isotopologues are removed preferentially. We hypothesize that our observed isotopic signatures are controlled by a temperature-dependent isotope equilibration process between H_2 and H_2O. The latter is the dominant pool of hydrogen in the exhaust as it is abundant at concentrations of ∼130 000 ppm and hence more than one order of magnitude larger than any other hydrogen-containing compounds in the lambda range of interest, including H_2. For such an equilibration process, the hotter engine exhaust (∼ 800 − 1000°C) results in a higher isotope ratio compared to the relatively cooler exhaust (∼ 500 − 700°C) downstream of the TWC (Bottinga, 1969). A similar temperature-dependent isotope equilibration process was recently suggested by Affek and Eiler (2006) for the oxygen isotopes in CO_2 and H_2O in car exhaust and by Rahn et al. (2002) for H_2–H_2O in high-temperature steam reforming and low-temperature photobiological processes.

To explore the above hypothesis we investigate whether the post-TWC samples at the different TWC temperatures of the 4 operating modes show this equilibration effect. In Fig. 2 we compare the isotope ratios of the post-TWC fuel-rich samples with results from the theoretically derived H_2 – H_2O isotope equilibrium as studied by Bottinga (1969). We plot the isotope results as a function of the exhaust temperature ranges as measured before and after the TWC. For a direct comparison of our results to those of Bottinga (1969) the δ values should be reported relative to the H_2O with which the H_2 is in equilibrium but unfortunately H_2O was not collected for isotope analysis. However, as the H_2O is the dominant hydrogen pool in the exhaust, its δD can be approximated by that of the gasoline, which is estimated at –80‰ to −110‰ vs. VSMOW (Schimmelmann et al., 2006). We therefore convert the theoretical results (Bottinga, 1969) to the VSMOW scale by shifting them by these offsets (Fig. 2). Our measured δD values of the fuel-rich post-TWC samples then show a temperature-dependence that is very similar to that derived from theory (Fig. 2). This holds for the experiments with gasoline. The δD of the sample collected when CH_4 was used as fuel is offset by ∼80‰ from the range for gasoline. This finding is also consistent with our hypothesis because CH_4 in natural gas is even more depleted in D/H than gasoline, e.g. δD equals −190‰ to −220‰ vs. VSMOW for natural gas of Russian origin (Cramer et al., 1999), which accounts for a significant fraction of the European pipeline natural gas mixture from which the CH_4 in our experiment was extracted.

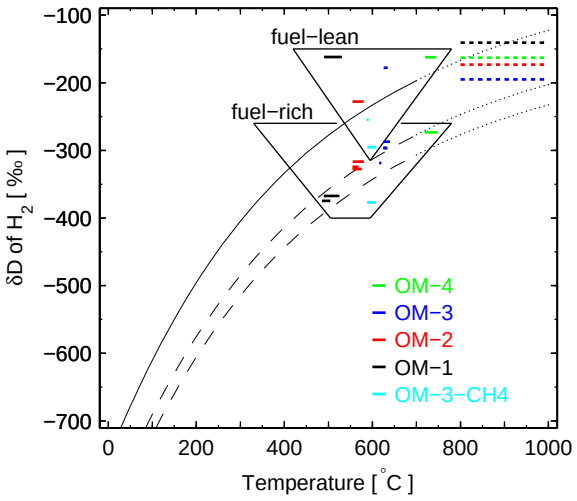

Fig. 2. Temperature-dependence of δD of H_2 produced in motor vehicle engine combustion. The short solid horizontal lines of variable size denote the δD in H_2 for various operating modes (see Fig. 1) on the VSMOW scale of the downstream three-way catalytic converter (post-TWC) exhaust samples. The width of the lines indicate the temperature ranges of the TWC. The solid curved line is a theoretical prediction (dotted lines is our extrapolation using a function $a + b \times T + c \times T^{1/2}$) of δD in H_2 in isotopic equilibrium with H_2O (Bottinga, 1969) and plotted relative to δD of H_2O as a reference. This curved line is shifted by the estimated δD of H_2O in gasoline exhaust (−80‰ to −110‰ vs. VSMOW, (Schimmelmann et al., 2006), dashed curved lines) in order to match the scale of reference. The fuel-rich post-TWC gasoline δD agree well with the predicted values. The results for the pre-TWC samples are plotted as dashed lines in the upper right corner in the approximate temperature range of the exhaust gas when exiting the engine.

In the above evaluation, we have ignored the hydrogen added to the system from the water in the intake air. At $\lambda = 1$, the H_2O concentration of the intake air contributes to ∼10 % to the total hydrogen pool. This is calculated based on the relative humidity in the air intake, which is controlled at 50 %, and the measured H_2O in the exhaust, which is the dominant hydrogen contribution in the exhaust. Because this experiment was conducted during a cold season (January), the intake air had to be moisturized (rather than dried) to maintain it at 50 % humidity. This was done by adding local tap water, with an isotope ratio likely to be in the range $\delta D = -50$‰ to −100‰ (Schürch et al., 2003). This is close to the isotopic composition of gasoline used above, and taking this additional hydrogen source into account would shift the line in Fig. 2 by <5 ‰. This shift is small compared to the uncertainties in these calculations and we therefore exclude this correction from Fig. 2. Since methane is isotopically more depleted, the correction for the methane-fuelled engine would be larger, but still <15 ‰.

Our finding of an equilibration temperature similar to the temperature of the TWC is somewhat surprising. Exhaust flow is fast and so are its temperature changes. The H_2–H_2O isotopic equilibration rates at these high temperatures are assumed to be fast also, but likely to slow down as the exhaust cools. As a consequence, it is to be expected that the δD in H_2, which is also changing rapidly in the cooling exhaust stream, leads to a final mean δD, which is derived from a composite (frequency distribution) of isotope ratios from a wider equilibration temperature range, rather than a δD from a single equilibration temperature. The width of this temperature distribution remains however unclear, but is likely related to the rate of exhaust cooling and to geometry and surface area effects in the exhaust stream. Alternatively the mean δD can also be regarded as an equilibration in a narrow-width temperature distribution approximated by a single "lock-in" temperature. Although inconclusively, Affek and Eiler (2006) find evidence in their study that the oxygen isotope ratio in CO_2–H_2O corresponds to such a single lock-in temperature of $\sim 200\,^{\circ}C$, rather than a mixture of isotope ratios from a broad temperature spectrum (isotopic mean from e.g. 900 and 50 °C in their example). If in our case the system was also better characterized by a single lock-in temperature, it would certainly not be the same as that found by Affek and Eiler (2006) for CO_2–H_2O. In our case of H_2 – H_2O, a lock-in temperature of 200 °C would result in a theoretical $H_2-\delta D$ of approximately −600‰, a value that is inconsistent with our laboratory observations or any field observations of combustion/industrial isotope signatures found in the past (Begemann and Friedman, 1959; Ehhalt et al., 1963; Gerst and Quay, 2001; Gonsior and Friedman, 1962; Rahn et al., 2002). As shown above, the lock-in temperatures for the post-TWC fuel-rich samples in our experiment would be the TWC temperatures (∼500–700 °C). This suggests that, in the case of H_2–H_2O, the TWC catalytic activity facilitates a rapid isotope equilibration and that a potential isotopic re-adjustment at lower temperatures downstream of the TWC is insignificant. In contrast, the finding of Affek and Eiler (2006) suggests that for CO_2–H_2O, the lock-in of the isotope equilibration occurs well downstream of the TWC at much lower temperatures.

In Fig. 2, we also indicated the $H_2-\delta D$ of our pre-TWC results by plotting these in the temperature range that is typical for exhaust gases leaving the engine's combustion chamber (800–1000 °C). Qualitatively, the observation that these δD values are higher than those from the post-TWC samples again supports the temperature hypothesis, but quantitatively the δD values are more enriched for the respective temperatures than expected from theory. For the δD of these samples, the lock-in temperature would need to be much higher. The present study cannot resolve whether these signatures could be the remnants of H_2–H_2O equilibration at the much higher temperatures (up to ∼2300 °C) during the combustion process.

2.5 H_2 isotope fractionation during catalytic removal

The temperature-driven H_2–H_2O isotope equilibration, as discussed in the previous section, can only explain some of the $H_2-\delta D$ variability we measured. For the individual operating modes, we observe a strong dependence of the isotope ratios on λ, particularly in the fuel-lean range (Fig. 1), even though there is only minor TWC temperature variability for each individual operating mode. δD of H_2 increases with increasing λ (Fig. 1). To characterize the isotopic enrichment during H_2 removal, we estimate the fractionation using the Rayleigh model where we relate the changes in δD to the fraction f of the post-TWC to the initial (pre-TWC) H_2 concentrations (e.g. Kaiser et al., 2002):

$$\ln(1+\delta D_{\mathrm{res}}) = \ln(1+\delta D_0) + \varepsilon \times \ln(f) \quad (1)$$

where δD_{res} and δD_0 are the post (residual) – and pre-TWC δD values of H_2, respectively, and ε is the enrichment factor. Note that a δD value of e.g. −300‰ (arbitrary number) has to be entered as −0.3 in Eq. (1). Also, because of the large isotope variations we refrain from the conventional linear approximation $\ln(\delta D + 1) \approx \delta D$. For our arbitrary example this means that the $\delta D = -300$ ‰ corresponds to $\ln(\delta D + 1) = -357$ ‰. The ε is related to the fractionation factor α (defined as the ratio of the reaction/removal rates, $\alpha = k(HD)/k(H_2)$) through the definition $\varepsilon = (\alpha - 1)$ and usually expressed in ‰, see (e.g. Friedman and O'Neil, 1977; Brenninkmeijer et al., 2003). The ε is calculated using least-square fitting techniques and is graphically shown in Fig. 3. We fit the data by linear regression, but in a first run we exclude the results for the very low H_2 concentration samples ($\ln(f) \approx -10$) because due to their very low H_2 concentrations, any potential contamination with ambient air or isotope effects other than that discussed here, would have strong influences on the δD (the large uncertainty in these samples' H_2 concentrations is relatively small when plotted on a logarithmic scale). For the linear regressions of OM-2 and OM-3, we find $R^2 \approx 0.6$ each and large 95% confidence bands. The linear regressions for these operating modes and for OM-1 (dashed lines in Fig. 3) closely predict the results at the low ln(f) end. This enhances the confidence that these samples may not have been altered significantly by any potential contamination, and we therefore include them in the linear regression (solid lines). This results in the following fractionation constants for the different operating points with 95% confidence bands: for $\varepsilon_{\mathrm{OM-1}} = -39.8 \pm 3.1$‰, $\varepsilon_{\mathrm{OM-2}} = -15.5 \pm 3.0$‰, $\varepsilon_{\mathrm{OM-3}} = -18.8 \pm 5.2$‰ ($R^2 > 0.98$ for all fits), and the slope of the line connecting the two OM-4 samples yields $\varepsilon_{\mathrm{OM-4}} = -16.7$‰. For the methane-fuelled experiment OM-4-CH_4, we calculate a fractionation constant of $\varepsilon_{\mathrm{OM-4-CH4}} = -20.2 \pm 69$‰.

Our analysis thus suggests the presence of two separate isotope effects, a H_2–H_2O temperature-dependent isotope equilibration, and a kinetic isotope fractionation during H_2

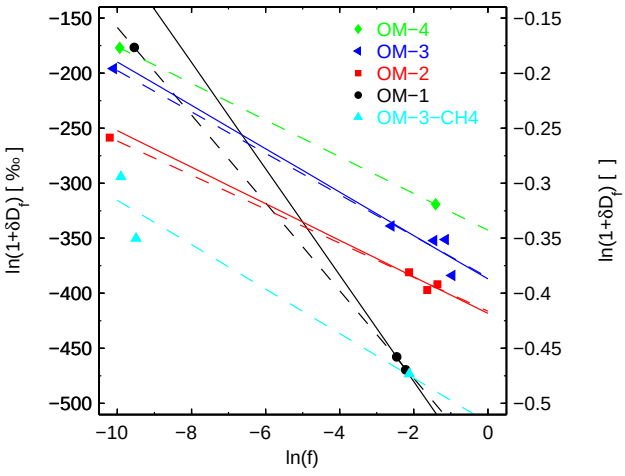

Fig. 3. Rayleigh fractionation diagram for the δD-H_2 isotope fractionation of post-catalytic converter exhaust of a car engine. The solid lines are least-square linear fits through the data excluding those with low ln(f) near −10, and the dashed lines are linear fits using all data points. The five colors denote different operating modes of the engine (see Fig. 1).

removal. While our observations can be fully explained by these two mechanisms, it is the simultaneous appearance of both effects in our samples that remains puzzling. Since H_2 removal is largely bound to the TWC surface, this is the place where the kinetic isotope fractionation is believed to occur during the ∼100 ms residence time in the TWC. The H_2–H_2O equilibration step must, however, also mainly occur in the TWC. This is obvious from the strong isotopic depletion when comparing post-TWC with corresponding pre-TWC isotope results. It is unlikely that the H_2–H_2O isotope equilibration would occur downstream of the TWC, as this would remove the clear isotopic signatures related to fractionation during removal. It is more likely that the equilibrium fractionation sets the general δD value at the TWC temperature, and subsequently there is a kinetic process that removes H_2 with the stated kinetic isotope effect. It should also be noted that the temperature of the exhaust gas increases by ∼ 50°C during passage through the TWC due to the exothermic reactions (the TWC is not actively heated). Given this, it is even more surprising to find the results of both effects downstream of the TWC. TWC chemistry is very complex also with regard to H_2, and it is therefore also possible that some additional processes and fractionations may potentially influence our results. Hydrocarbon steam-reforming and partial oxidation, water-gas shift reaction, NO-reduction, and H_2 oxidation by O_2 are some of the processes involving hydrogen (D. Ferri pers. communication, Salaün et al. (2009)).

2.6 Exhaust ratios of H_2/CO, H_2/CO_2 and CO/CO_2

The ratios of H_2/CO, H_2/CO_2 and CO/CO_2 (in this paper reported on a molar basis) in traffic exhaust have recently received increased attention because of their potential to identify and characterize traffic pollution events in atmospheric observations, and to up-scale traffic emissions using the better constrained emission inventories of CO and CO_2. Many studies over the past decades have revealed tight H_2 to CO relationships in raw engine exhaust (D'Alleva and Lovell, 1936; Leonard, 1961; Auckenthaler, 2005) and our pre-TWC H_2/CO of 0.2–0.35 (Figs. 1 and 4) are in close agreement with these findings. Recent field studies of anthropogenically polluted air in Europe and North America have shown H_2/CO ratios to vary in a relatively narrow range of ∼0.3–0.6 (Novelli et al., 1999; Barnes et al., 2003; Steinbacher et al., 2007; Aalto et al., 2009), and when the traffic component was isolated from other H_2 and CO sources and sinks, yielded ratios of 0.48–0.51 (Vollmer et al., 2007; Hammer et al., 2009). Our post-TWC results show considerable variability (Figs. 1 and 4) for the four operating modes and the λ settings. In the fuel-rich range, H_2/CO varied between 0.05 and 1.6 depending on the operating mode (with coolest TWC exhibiting the lowest ratios). Surprisingly the H_2/CO reduced to about half for the actively-cooled TWC (OM-1 vs. OM-2) which is due to reduced H_2 emissions. H_2/CO increases significantly near λ=1. However, for λ ≥1 the H_2 and CO concentrations are tagged with high measurement uncertainties and consequently their ratios have large errors, and we are not further discussing these here. From an integrative aspect, because of their low concentrations, these ratios are also less important as they quantitatively add little to the overall traffic exhaust in a real-world case. In light of a comparison with real-world emissions, a more robust measure of H_2/CO is the cumulative H_2/CO. The overall cumulative H_2/CO over all gasoline post-TWC measurements is 0.25, about half of that observed in an integrative tunnel study (0.51±0.11, Vollmer et al. (2007)). This difference is likely caused by the somewhat arbitrary selection of λ-points which affects our cumulative estimate, and the generally large variability found throughout individual single-vehicle exhaust systems (Bond et al., 2010). Differences may also occur because our study uses more static settings compared to the dynamics found in real traffic. This is likely to cause some differences in the regime of O_2 storage capacities and hence may influence H_2 and CO levels too.

Our similarly-calculated overall ratio for H_2/CO_2 is 8.9×10^{-3}, about double that found in the tunnel study ($4.4\pm1.7\times10^{-3}$, Vollmer et al. (2007)), and likely caused by the low-H_2 high-CO_2 diesel exhaust component in the tunnel. We also relate the H_2/CO to the combustion efficiency, here defined as CO/CO_2 (Fig. 4). Although the overall cumulative combustion efficiency in our experiment is significantly higher than in the tunnel study (36×10^{-3} vs. $8.4\pm2.8\times10^{-3}$), these results demonstrate the generally

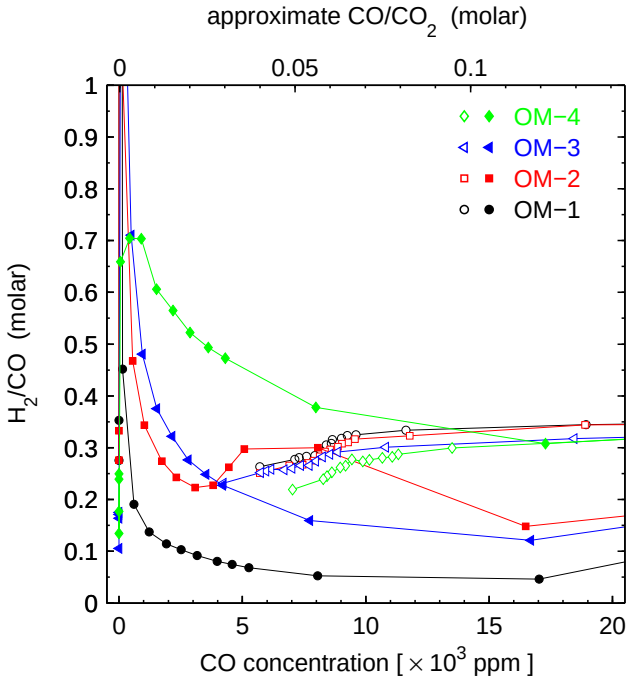

Fig. 4. Molar H_2/CO ratio plotted vs. CO concentration. Open symbols denote pre-TWC samples and filled symbols denote post-TWC samples. The color-coding is the same as in Fig. 1.

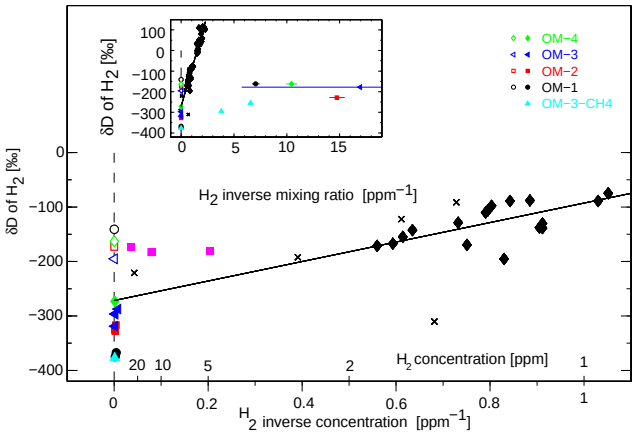

Fig. 5. Isotope ratio δD-H_2 vs. inverse concentration (Keeling plot). The open and filled symbols on the vertical dashed line denote pre- and post-catalytic converter samples, respectively. The color coding is the same as in Fig. 1. The black crosses (single vehicles) and diamonds (city air) are from a study in the Los Angeles Basin by Rahn et al. (2002) with a fit (solid line) through their data pointing to a −270‰ isotopic end-member. The magenta squares are from samples taken in a parking garage by Gerst and Quay (2001). The insert includes the additional sub-ambient concentration samples of the post-catalytic lean engine combustion.

more efficient combustion in vehicle engines compared to biomass burning (e.g., Röckmann et al., 2010). These findings suggest that the simultaneous determination of H_2, CO, and CO_2, possibly along with isotopic measurements, may provide a tool to distinguish traffic exhaust from biomass burning in air pollution.

2.7 Implications for real-world emissions

Although here we present results from a single engine/TWC experiment, some results are likely applicable to other engine settings and to real-world driving conditions. For the investigated engine, H_2 removal by the TWC is large. This implies that single motor vehicle H_2 emissions from traffic have decreased strongly since the introduction of the catalytic converter in the 1970s. Due to increasingly stringent emission legislation around the world, improvements in catalytic converter technology, engine fueling precision, and the development of lambda control algorithms, global traffic H_2 and CO emissions are expected to decrease despite the increasing global car fleet (Vollmer et al., 2007).

To place our isotope results in a real-world context, we compare these to earlier published D/H isotope measurements of air samples polluted with traffic exhaust. This comparison is shown in Fig. 5 as a "Keeling" plot, where the isotopic signature is plotted against the inverse concentration of the sample. Rahn et al. (2002) have measured traffic-polluted air samples in the Los Angeles basin in 2000, from which they derived a integrated pure anthropogenic isotopic signature (end-member) of −270‰. This extrapolated value is bracketed by our pre-TWC and fuel-rich post-TWC results. Earlier results from Gerst and Quay (2001) from samples taken in 1999 in a parking garage in Seattle yielded higher concentration samples than those by Rahn et al. (2002), and were less depleted in D/H with results ranging from −173‰ to −183‰. The insert of Fig. 5 also includes the samples with very low concentrations from the fuel-lean range. As these concentrations are sub-ambient, they cannot be quantitatively investigated in the Keeling diagram. Still, the isotope signatures are in the same range as the very high concentration samples. This suggests that in fact all of our samples are "pure" end-member samples (not mixtures of produced H_2 with ambient background H_2), but with largely differing source strengths.

On the one hand, all of our high-concentration post-TWC results show a δD equal or more negative than the end-member value predicted by Rahn et al. (2002), with the signature from the cooled TWC of OM-1 (and from the methane-powered engine) showing the largest depletion of about −370‰. On the other hand, all of our pre-catalytic converter results show isotopic ratios that are much more enriched compared to the predicted end-member of −270‰. These samples do, however, agree well with the results from Gerst and Quay (2001) from a parking garage in Seattle.

An interpretation of our results from a fleet-level perspective may provide some explanations for these apparent discrepancies. The isotopic signatures of exhaust at $\lambda>1$ are probably of little quantitative relevance because the H_2 concentrations are very small. In contrast, emissions during cold starts and in the fuel-rich range ($\lambda<1$) are large, and hence their isotopic signatures are of importance. Emissions from single vehicle studies of standardized driving cycles show that cold start H_2 emissions can contribute up to 40% of the cycles' total emissions (Bond et al., 2010). The extrapolated end-member of -270‰ by Rahn et al. (2002) based on their Los Angeles Basin study is likely a regional mixture of emissions from cold-starts (thus pre-TWC signatures) on the one hand (>-270‰) and fuel-rich TWC emissions (<-270‰) on the other. Because cold-start emissions are expected to continue contributing significantly to overall vehicle emissions, it is likely that the end-member value of -270‰ (Rahn et al., 2002) will be a useful average value for developed countries. For developing countries however, with parts of their fleets not equipped with TWC, it is likely that the high emissions from non-TWC vehicles will lead to a higher mean δD in H_2 traffic emissions.

It is tempting to attribute the relatively elevated δD found by Gerst and Quay (2001) to an apparent unrepresentative sampling location, since samples in a parking garage may be biased towards cold-start emissions (thus pre-TWC signatures). However Gerst and Quay (2001) state that their samples were taken in the morning when the majority of the vehicles arrive at the parking garage (presumably with fully-functional TWCs). Still the high emissions of a few potential cold-starts (with higher isotopic ratio) in the parking garage may have significantly influenced their results.

3 Conclusions

If our results are representative of a large variety of vehicle engine/TWC systems, then our findings have several implications. Our results suggest that the isotopic signatures from vehicle emissions have "lightened" over the last decades due to the introduction of catalytic converters in the 1970s. It is likely that this evolution has progressed in different manners in different regions of the world. Assuming that the majority of the third-world countries converted to TWC technology at a slower rate than industrialized countries, this would imply that there may have been (and still could be) a geographical difference in the isotopic signature of traffic exhaust. Our results also suggest that traffic sampling should be carried out with caution. Urban traffic with more frequent congested traffic used to be characterized by more fuel-rich conditions with high H_2 emissions hence probably lower isotope ratios. Current technological developments, however, avoid fuel-rich driving in urban traffic due to better lambda control systems, hence the fuel-rich driving (and thereby the low isotope ratios) may be limited to very high speed driving (e.g. German highways). The isotopic signature of cold-start emissions may resemble engine exhaust without TWC, hence parking garages may yield relatively enriched isotopic signatures.

Because the TWC is not actively heated, its temperature is partially a reflection of the exhaust gas temperature reaching the TWC. Therefore the driving mode will affect the TWC temperature, which in turn results in largely differing emissions of H_2 concentrations, their δD-H_2 and H_2/CO ratio. However TWC and exhaust system geometry in combination with ambient temperatures will also significantly affect TWC temperatures and hence the emitted trace gases. Our results suggest that the exhaust δD-H_2 for colder ambient air (e.g. winter) hence cooler TWC is significantly more negative compared to warmer air (e.g. summer). Consequently, temperature variations should also lead to seasonal and geographical variations in δD-H_2, with, e.g., the tropics showing different exhaust signatures compared to the high latitudes. Exhaust geometry, air flow and ambient temperatures may easily lead to temperature differences similar to the ~ 50°C found for our OM-1 and OM-2 experiments, and could therefore lead to variability of δD-H_2 of $\sim$50‰. Further studies are needed to fully confirm the hypothesis of a temperature-driven isotopic H_2-H_2O equilibration in motor vehicle exhaust and the potential variability caused by catalytic converters, exhaust geometry, and ambient temperature conditions. Studies on a fleet level (e.g. tunnel studies) in various seasons and parts of the world could greatly help to better characterize the H_2 traffic emissions and their isotopic signatures.

Except for the study by Affek and Eiler (2006), other isotope studies of car exhaust do not specifically address the question whether a significant thermal equilibration process between H_2O and other exhaust compounds may occur. Combined pre- and post-TWC measurements were generally not conducted except for the N_2O study by Toyoda et al. (2008). In their study, both isotopic enrichment and depletion were observed across the TWC, depending on the settings of the experimental variables, but in their case, the situation is complicated by both destruction and production of N_2O in the exhaust stream. For CH_4 and CO stable isotope studies on cars, including one without catalytic converter (Nakagawa et al., 2005; Tsunogai et al., 2003), there is no clear evidence of thermal hydrogen or oxygen equilibration with H_2O, possibly because of the overwhelming kinetic isotope fractionation during catalytic removal of CH_4 and CO. However, in the exhaust of the car without catalytic converter, Tsunogai et al. (2003) find ^{18}O-depletion (but no ^{13}C depletion) in CO when the engine is still relatively cold compared to when it is hot. It remains unclear whether this could also be a thermal equilibration effect between CO and H_2O, or, as the authors hypothesize, the cold-start is characterized by an O_2-depleted combustion (hence the large CO emissions) possibly resulting in an enhanced kinetic isotope effect during the atmospheric oxygen destruction stage thereby producing ^{18}O

depleted CO. It is possible that the biomass burning ^{18}O depletion in CO of colder smoldering combustion stages compared to hotter flaming stages (Tsunogai et al., 2003) could be partially caused by thermal equilibration processes with H_2O or O_2. Similarly, for biomass burning (Röckmann et al., 2010), the isotopic depletion in D/H with increasingly poor combustion efficiency ($\Delta CO/\Delta CO_2$) may ultimately be partially related to temperature effects because poor combustion efficiency is generally related to lack of oxygen and hence to lower-temperature combustion.

Acknowledgements. We acknowledge partial support for this study by the European Union framework program FP6-2005-Global-4 (EuroHydros) and the "Competence Center for Energy and Mobility", Switzerland (CCEM-CH). S. Walter was supported by the project "H_2 budget" of the Dutch national science foundation NWO (grant 816-01-001). Rolf Ziegler and Roland Graf have significantly contributed to the experimental part of this study.

Edited by: P. O. Wennberg

References

Aalto, T., Lallo, M., Hatakka, J., and Laurila, T.: Atmospheric hydrogen variations and traffic emissions at an urban site in Finland, Atmos. Chem. Phys., 9, 7387–7396, doi:10.5194/acp-9-7387-2009, 2009.

Affek, H. P. and Eiler, J. M.: Abundance of mass $^{47}CO_2$ in urban air, car exhaust, and human breath, Geochim. Cosmochim. Acta, 70, 1–12, doi:10.1016/j.gca.2005.08.021, 2006.

Auckenthaler, T. S.: Modelling and Control of Three-Way Catalytic Converters, Ph.D. Thesis, Swiss Federal Institute of Technology, Zurich, No. 16018, 2005.

Barnes, D. H., Wofsy, S. C., Fehlau, B. P., Gottlieb, E. W., Elkins, J. W., Dutton, G. S., and Novelli, P. C.: Hydrogen in the atmosphere: Observations above a forest canopy in a polluted environment, J. Geophys. Res., 108(D6), 4179 doi:10.1029/2001JD001199, 2003.

Begemann, F. and Friedman, I.: Tritium and deuterium content of atmospheric hydrogen, Z. Naturforsch. A, 14, 1024–1031, 1959.

Bond, S. W., Alvarez, R., Vollmer, M. K., Steinbacher, M., Weilenmann, M., and Reimann, S.: Molecular hydrogen (H_2) emissions from gasoline and diesel vehicles, Sci. Tot. Environ., 408, 3596–3606, 2010.

Bottinga, Y.: Calculated fractionation factors for carbon and hydrogen isotope exchange in system calcite-carbon dioxide-graphite-methane-hydrogen-water vapor, Geochim. Cosmochim. Acta, 33, 49–64, 1969.

Brenninkmeijer, C. A. M., Janssen, C., Kaiser, J., Röckmann, T., Rhee, T. S., and Assonov, S. S.: Isotope effects in the chemistry of atmospheric trace compounds, Chem. Rev., 103, 5125–5161, doi:10.1021/cr020644k, 2003.

Brühlmann, S.: Validierung H-Sense, Tech. Rep. unpublished, Empa, Swiss Federal Laboratories for Materials Testing and Research, 2004.

Chanton, J. P., Rutkowski, C. M., Schwartz, C. C., Ward, D. E., and Boring, L.: Factors influencing the stable carbon isotopic signature of methane from combustion and biomass burning, J. Geophys. Res., 105(D2), 1867–1877, 2000.

Craig, H.: Standards for reporting concentrations of deuterium and oxygen-18 in natural waters, Science, 133, 1833–1834, 1961.

Cramer, B., Poelchau, H. S., Gerling, P., Lopatin, N. V., and Littke, R.: Methane released from groundwater: the source of natural gas accumulations in northern West Siberia, Marine Petrol. Geol., 16, 225–244, 1999.

D'Alleva, B. A. and Lovell, W. G.: Relation of exhaust gas composition to air-fuel ratio, SAE Journal, 38, 90–98, 1936.

Ehhalt, D., Israel, G., Roether, W., and Stich, W.: Tritium and deuterium content of atmospheric hydrogen, J. Geophys. Res., 68(13), 3747–3751, 1963.

Ehhalt, D. H. and Rohrer, F.: The tropospheric cycle of H_2: a critical review, Tellus, Ser. B., 61, 500–535, doi:10.1111/j.1600-0889.2009.00416.x, 2009.

Feilberg, K. L., Johnson, M. S., Bacak, A., Röckmann, T., and Nielsen, C. J.: Relative tropospheric photolysis rates of HCHO and HCDO measured at the European photoreactor facility, J. Phys. Chem. A, 111, 9034–9046, doi:10.1021/jp070185x, 2007.

Friedman, I. and O'Neil, J. R.: Compilation of stable isotope fractionation factors of geological interest, in: Data of Geochemistry, Geological Survey Professional Paper 440-KK, 6th edn., KK1–KK12, 1977.

Gerst, S. and Quay, P.: Deuterium component of the global molecular hydrogen cycle, J. Geophys. Res., 106(D5), 5021–5031, 2001.

Gonfiantini, R.: Standards for stable isotope measurements in natural compounds, Nature, 271, 534–536, 1978.

Gonsior, B. and Friedman, I.: Tritium and Deuterium im atmosphärischen Wasserstoff, Z. Naturforsch. A, 17, 1088–1091, 1962.

Hammer, S., Vogel, F., Kaul, M., and Levin, I.: The H_2/CO ratio of emissions from combustion sources: comparison of top-down with bottom-up measurements in southwest Germany, Tellus, Ser. B., 61, 547–555, 2009.

Haryanto, A., Fernando, S. D., Filip To, S. D., Steele, P. H., Pordesimo, L., and Adhikari, S.: Hydrogen production through the water-gas shift reaction: Thermodynamic equilibrium versus experimental results over supported Ni catalysts, Energy Fuel., 23, 3097–3102, doi:10.1021/ef801076r, 2009.

Hauglustaine, D. A. and Ehhalt, D. H.: A three-dimensional model of molecular hydrogen in the troposphere, J. Geophys. Res., 107(D17), 4330, doi:10.1029/2001JD001156, 2002.

Kaiser, J., Brenninkmeijer, C. A. M., and Röckmann, T.: Intramolecular ^{15}N and ^{18}O fractionation in the reaction of N_2O with $O(^1D)$ and its implications for the stratospheric N_2O isotope signature, J. Geophys. Res., 107(D14), 4214, doi:10.1029/2001JD001506, 2002.

Leonard, L. S.: Fuel distribution by exhaust gas analysis, Society of automobile engineers, 379A, 1–22, 1961.

Nakagawa, F., Tsunogai, U., Komatsu, D. D., Yamada, K., Yoshida, N., Moriizumi, J., Nagamine, K., Iida, T., and Ikebe, Y.: Automobile exhaust as a source of ^{13}C- and D-enriched atmospheric methane in urban areas, Organic Geochem., 36, 727–738, 2005.

Novelli, P. C., Lang, P. M., Masarie, K. A., Hurst, D. F., Myers, R., and Elkins, J. W.: Molecular hydrogen in the troposphere: global distribution and budget, J. Geophys. Res., 104(D23), 30427–30444, 1999.

Pieterse, G., Krol, M. C., and Röckmann, T.: A consistent molecular hydrogen isotope chemistry scheme based on an independent bond approximation, Atmos. Chem. Phys., 9, 8503–8529, doi:10.5194/acp-9-8503-2009, 2009.

Price, H., Jaeglé, L., Rice, A., Quay, P., Novelli, P. C., and Gammon, R.: Global budget of molecular hydrogen and its deuterium content: Constraints from ground station, cruise, and aircraft observations, J. Geophys. Res., 112, D22108, doi:10.1029/2006JD008152, 2007.

Rahn, T., Kitchen, N., and Eiler, J.: D/H ratios of atmospheric H_2 in urban air: Results using new methods for analysis of nano-molar H_2 samples, Geochim. Cosmochim. Acta, 66(14), 2475–2481, 2002.

Rahn, T., Eiler, J. M., Boering, K. A., Wennberg, P. O., McCarthy, M. C., Tyler, S., Schauffler, S., Donnelly, S., and Atlas, E.: Extreme deuterium enrichment in stratospheric hydrogen and the global atmospheric budget of H_2, Nature, 424, 918–921, 2003.

Rhee, T. S., Mak, J., Röckmann, T., and Brenninkmeijer, C. A. M.: Continuous-flow isotope analysis of the deuterium/hydrogen ratio in atmospheric hydrogen, Rapid Commun. Mass Spectrom., 18, 299–306, 2004.

Rhee, T. S., Brenninkmeijer, C. A. M., and Röckmann, T.: The overwhelming role of soils in the global atmospheric hydrogen cycle, Atmos. Chem. Phys., 6, 1611–1625, doi:10.5194/acp-6-1611-2006, 2006.

Röckmann, T., Rhee, T. S., and Engel, A.: Heavy hydrogen in the stratosphere, Atmos. Chem. Phys., 3, 2015–2023, doi:10.5194/acp-3-2015-2003, 2003.

Röckmann, T., Gómez Álvarez, C. X., Walter, S., van der Veen, C., Wollny, A. G., Gunthe, S., Helas, G., Pöschl, U., Keppler, F., Greule, M., and Brand, W. A.: The isotopic composition of H_2 from biomass burning-dependency on combustion efficiency, moisture content and δD of local precipitation, J. Geophys. Res., in review, 2010.

Salaün, M., Kouakou, A., Da Costa, S., and Da Costa, P.: Synthetic gas bench study of a natural gas vehicle commercial catalyst in monolithic form: On the effect of gas composition, Appl. Catalys. B: Environmental, 88, 386–397, 2009.

Sanderson, M. G., Collins, W. J., Derwent, R. G., and Johnson, C. E.: Simulation of global hydrogen levels using a Lagrangian three-dimensional model, J. Atmos. Chem., 46, 15–28, 2003.

Schimmelmann, A., Sessions, A. L., and Mastalerz, M.: Hydrogen isotopic (D/H) composition of organic matter during diagenesis and thermal maturation, Ann. Rev. Earth Planet. Sci., 34, 501–533, doi:10.1146/annurev.earth.34.031405.125011, 2006.

Schürch, M., Kozel, R., Schotterer, U., and Tripet, J.-P.: Observation of isotopes in the water cycle – the Swiss National Network (NISOT), Environ. Geol., 45, 1–11, 2003.

Steinbacher, M., Fischer, A., Vollmer, M. K., Buchmann, B., Reimann, S., and Hueglin, C.: Perennial observations of molecular hydrogen (H_2) at a suburban site in Switzerland, Atm. Environ., 41, 2111–2124, doi:10.1016/j.atmosenv.2006.10.075, 2007.

Toyoda, S., Yamamoto, S., Arai, S., Nara, H., Yoshida, N., Kashiwakura, K., and Akiyama, K.: Isotopomeric characterization of N_2O produced, consumed, and emitted by automobiles, Rapid Commun. Mass Spectrom., 22, 603–612, doi:10.1002/rcm.3400, 2008.

Tsunogai, U., Hachisu, Y., Komatsu, D. D., Nakagawa, F., Gamo, T., and Akiyama, K.: An updated estimation of the stable carbon and oxygen isotopic compositions of automobile CO emissions, Atmos. Environ., 37(35), 4901–4910, doi:10.1016/j.atmosenv.2003.08.008, 2003.

Vollmer, M. K., Juergens, N., Steinbacher, M., Reimann, S., Weilenmann, M., and Buchmann, B.: Road vehicle emissions of molecular hydrogen (H_2) from a tunnel study, Atmos. Environ., 8355–8369, 41(37), doi:10.1016/j.atmosenv.2007.06.037, 2007.

Walter, S. and et al.: Manuscript in preparation, 2010.

Xiao, X., Prinn, R. G., Simmonds, P. G., Steele, L. P., Novelli, P. C., Huang, J., Langenfelds, R. L., O'Doherty, S., Krummel, P. B., Fraser, P. J., Porter, L. W., Weiss, R. F., Salameh, P., and Wang, R. H. J.: Optimal estimation of the soil uptake rate of molecular hydrogen from the Advanced Global Atmospheric Gases Experiment and other measurements, J. Geophys. Res., 112, D07303, doi:10.1029/2006JD007241, 2007.